CHEMISTRY OF MATERIALS
Article

Chem. Mater. **2009,** *21,* 4925–4933 4925
DOI:10.1021/cm902206q

Phenyl@Rh(I)-Bridged Periodic Mesoporous Organometalsilica with High Catalytic Efficiency in Water-Medium Organic Reactions

Xushi Yang,[†] Fengxia Zhu,[‡] Jianlin Huang,[‡] Fang Zhang,[‡] and Hexing Li*[,†,‡]

[†]*Chemical and Molecular Engingeering School, East China University of Science and Technology, Shanghai 200237, China, and* [‡]*Department of Chemistry, Shanghai Normal University, Shanghai 200234, China*

Received May 25, 2009. Revised Manuscript Received September 8, 2009

A facile approach to prepare phenyl and Rh(I) organometal bridged periodic mesoporous organometalsilica was developed based on surfactant-directed co-condensation of $RhCl[PPh_2(CH_2)_2Si(OEt_3)_3]_3$ and $(OEt)_3SiPhSi(OEt)_3$. The as-prepared Rh(I)-PPh_2-PMO(Ph) exhibited matchable catalytic efficiency with the corresponding $Rh(PPh_3)_3Cl$ homogeneous catalyst in water-medium reaction between phenylboronic acid and butyl acrylate or the 1,4-conjugate addition reaction between phenylboronic acid and *N*,*N*-dimehytlacyrlmaide, which could be attributed to the high dispersion of Rh(I) active sites, the ordered mesoporous channels and the strong surface hydrophobicity resulting from phenyl fragments embedded in silica walls, leading to the facilitated the diffusion and the adsorption of organic molecules onto the catalyst in aqueous solution. The Rh(I)-PPh_2-PMO(Ph) could be used repetitively, showing the excellent durability that could be attributed to the effective inhibition of Rh(I) leaching and the high hydrothermal stability of the mesoporous structure.

Introduction

In the past two decades, mesoporous materials have been widely studied because of their potential applications in adsorption, chromatography, gas storage, and catalysis.[1−3] To date, the compositions of mesoporous materials have expanded from silicas[4,5] to carbon,[6] metal oxides,[7] metal sulfides,[8] and even polymers.[9] Recently, organic−inorganic hybrid silicas have received increasing attention because of the combined advantages from both the organic and inorganic functionalities.[10] The periodic mesoporous organosilicas (PMOs)[11] with organic fragments embedded in the silica walls are among the most often studied organic−inorganic hybrid silicas because of the well-defined ordered mesoporous structure and the uniform distribution of organic groups in the pore walls. Up to now, many PMOs containing ethyl-, 2-butylene-,[12] phenyl-, ethane-,[13] and biphenyl-groups[14] have been synthesized. However, to the best of our knowledge, the mesoporous periodic organometalsilica with both the organometal and organic fragments incorporated into silica framework have never been reported so far.

Organometallic catalysts have been widely used in organic syntheses, and the $Rh(PPh_3)_3Cl$, known as Wilkinson's catalyst, represents a typical example.[15−19] Recently, they are also employed in water-medium organic reactions, which could diminish environmental pollution from organic solvents.[20−23] Though the high activity and selectivity, the homogeneous organometallic catalysts usually show disadvantages in separation and recycling

*Corresponding author. E-mail: hexing-li@shnu.edu.cn.

(1) Kresge, C. T.; Leonowicz, M. E.; Roth, W. J.; Vartuli, J. C.; Beck, J. S. *Nature* **1992**, *359*, 710–712.
(2) Beck, J. S.; Vartuli, J. C.; Roth, W. J.; Leonowicz, M. E.; Kresge, C. T.; Schmitt, K. D.; Chu, C. T. W.; Olsen, D. H.; Sheppard, E. W. *J. Am. Chem. Soc.* **1992**, *114*, 10834–10843.
(3) Fujita, S.; Inagaki, S. *Chem. Mater.* **2008**, *20*, 891–908.
(4) Monnier, A.; Schüth, F.; Huo, Q.; Kumar, D.; Margolese, D.; Maxwell, R. S.; Stucky, G.; Krishnamurty, M.; Petroff, P.; Firouzi, A.; Janicke, M.; Chmelka, B. F. *Science* **1993**, *261*, 1299–1303.
(5) Zhao, D. Y.; Feng, J. L.; Huo, Q. H.; Melosh, N.; Fredrickson, G. H.; Chmelka, B. F.; Stucky, G. D. *Science* **1998**, *279*, 548–552.
(6) Meng, Y.; Gu, D.; Zhang, F. Q.; Shi, Y. F.; Cheng, L.; Feng, D.; Wu, Z. X.; Chen, Z. X.; Wan, Y.; Stein, A.; Zhao, D. Y. *Chem. Mater.* **2006**, *18*, 4447–4464.
(7) Tian, Z. R.; Tong, W.; Wang, J. Y.; Duan, N. G.; Krishnan, V. V.; Suib, S. L. *Science* **1997**, *276*, 926–930.
(8) MacLachlan, M. J.; Coombs, N.; Ozin, G. A. *Nature* **1999**, *397*, 681–684.
(9) Lu, Y. F. *Angew. Chem., Int. Ed.* **2006**, *45*, 7664–7667.
(10) Inagaki, S.; Guan, S.; Fukushima, Y.; Ohsuna, T.; Terasaki, O. *J. Am. Chem. Soc.* **1999**, *121*, 9611–9614.
(11) Inagaki, S.; Guan, S.; Ohsuna, T.; Terasaki, O. *Nature* **2002**, *416*, 304–307.
(12) Lu, Y. F.; Fan, H. Y.; Doke, N.; Loy, D. A.; Assink, R. A.; LaVan, D. A.; Brinker, C. J. *J. Am. Chem. Soc.* **2000**, *122*, 5258–5261.
(13) Hatton, B. D.; Landskron, K.; Whitnall, W.; Perovic, D. D.; Ozin, G. A. *Adv. Funct. Mater.* **2005**, *15*, 823–829.
(14) Kapoor, M. P.; Yang, Q. H.; Inagaki, S. *J. Am. Chem. Soc.* **2002**, *124*, 15176–15177.
(15) Osborn, L. A.; Jardine, F. H.; Young, J. F.; Wilkinson, G. *J. Chem. Soc. A* **1966**, 1711–1732.
(16) Shoai, S.; Bichler, P.; Kang, B.; Buckley, H.; Love, J. A. *Organometallics* **2007**, *26*, 5778–5781.
(17) Fukumoto, Y.; Kinashi, F.; Kawahara, T.; Chatani, N. *Org. Lett.* **2006**, *8*, 4641–4643.
(18) Zou, G.; Wang, Z. Y.; Zhu, J. R.; Tang, J. *Chem. Commun.* **2003**, 2438–2439.
(19) Dufaud, V.; Beauchesne, F.; Bonneviot, L. *Angew. Chem., Int. Ed.* **2005**, *44*, 3475–3477.
(20) Li, C. J. Chan, T. H. *Organic Reactions in Aqueous Media*; Wiley: New York, 1997.
(21) Lindstrom, U. M. *Chem. Rev.* **2002**, *102*, 2751–2772.
(22) Li, C. *J. Chem. Rev.* **2005**, *105*, 3095–3166.
(23) Hayashi, Y. *Angew. Chem., Int. Ed.* **2006**, *45*, 8103–8104.

Published on Web 09/30/2009

Scheme 1. Illustration of the Preparation of the Rh(I)-PPh_2-PMO(Ph) by Surfactant-Directed Co-Condensation

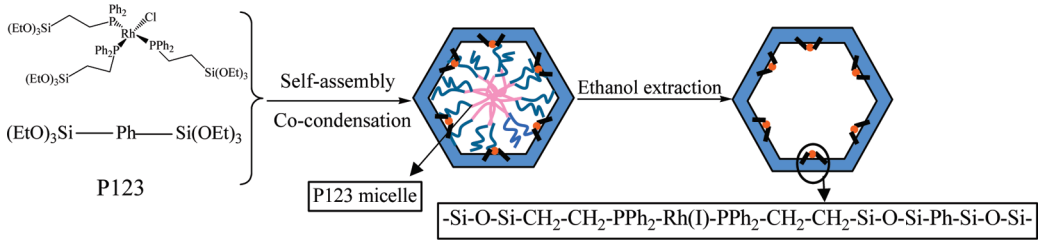

uses, which eventually add cost and even cause environmental pollution from heavy metallic ions.[24,25] Immobilized organometallic catalyst could effectively solve the above problems, however, their industrial applications are still quite limited by the poor activity and selectivity.[26−30] Previously, we reported the organometallic catalysts anchored on the mesoporous silica support with high dispersion degree of active sites. Meanwhile, functionalization with organic groups was also performed to enhance surface hydrophobicity, which promoted the diffusion and adsorption of organic molecules on the catalysts, especially in aqueous medium.[31−33] However, the introduction of the organometal and organic group by grafting method inevitably caused blockage of mesopore channels, leading to the reduced catalytic efficiency due to the diffusion limit. Meanwhile, these catalysts usually displayed poor durability because of the leaching of Rh(I) active sites during reactions. Herein, we report a novel heterogeneous Rh(I) organometallic catalyst prepared by surfactant-directed co-condensation of Rh(I) organometal-bridged silane and phenyl-bridged silane, denoted as Rh(I)-PPh_2-PMO(Ph). Both the Rh(I) organometal and the phenyl groups were homogeneously incorporated into the silica framework, leading to the well-defined ordered mesoporous channels and strong interaction of the Rh(I) active sites with the silica support. As a result, this catalyst exhibited high efficiencies and strong durability in water-medium reaction between phenylboronic acid and butyl acrylate (reaction 1) and 1,4-conjugate addition reaction between phenylboronic acid and *N*,*N*-dimehytlacyrlmaide (reaction 2), showing good potential in industrial applications.

Experimental Section

Catalyst Preparation. The formation of the phenyl and Rh(I) organometal bridged periodic mesoporous organometalsilica, denoted as Rh(I)-PPh_2-PMO(Ph), is illustrated in Scheme 1. First, a Rh(I) organometallicsilane was synthesized in a dry and oxygen-free argon atmosphere using Schlenk techniques.[34] In a typical run of synthesis, 2.7 mL of 2-(diphenylphosphino)-ethyltriethoxysilane [$PPh_2CH_2CH_2Si(OEt)_3$] was added slowly into 15 mL of anhydrous toluene containing 0.54 g o [Rh-(COD)Cl]$_2$. After the solution was stirred for 24 h at 298 K, the color changed from red-orange to red, the toluene was evaporated and the viscous residue was dissolved in 25 mL of anhydrous hexane. After cooling to 253 K, dark red oil was obtained that was dried at 333 K under vacuum. According to ICP analysis and ^{1}H NMR (CD_2Cl_2) analysis (see Figure 1): 7.2−7.5, 7.6−7.8 (3 m, 30 H, ArH), 3.7 (m, 18 H, OCH_2), 2.5 (m, 6 H, CH_2P), 1.1 (m, 27 H, CH_3), 0.79 (m, 6 H, $SiCH_2$), the composition was determined as $RhCl[PPh_2(CH_2)_2Si(OEt_3)_3]_3$. Then, the $RhCl[PPh_2(CH_2)_2Si(OEt_3)_3]_3$ in 1.0 mL of THF was mixed with 40 mL o f0.20 M HCl aqueous solution containing a certain amount of bis(triethoxysilyl) benzene [$(OEt)_3SiPhSi(OEt)_3$], 1.0 g of P123 and 3.0 g of KCl, which has prehydrolyzed for 40 min at 313 K. The initial molar ratio in the mother solution is Si:P123:KCl:HCl:H_2O = 1.0:0.017:4.0:0.80:218, where Si refers to the total silica source. After being stirred at 313 K for 24 h and aged at 373 K for another 24 h, the precipitate was filtrated and dried under a vacuum overnight. Finally, the surfactants and other organic substances were extracted and washed away by refluxing in ethanol solution for 24 h, leading to the Rh(I)-PPh_2-PMO(Ph) catalyst. The Rh(I) loading was adjusted by changing the amount of $RhCl[PPh_2(CH_2)_2Si(OEt)_3]_3$ in the initial mixture, corresponding to Rh(I)-PPh_2-PMO(Ph)-1, Rh(I)-PPh_2-PMO(Ph)-2, and Rh(I)-PPh_2-PMO(Ph)-3. According to ICP analysis, the real Rh(I) loadings in these three catalysts were determined as 0.019, 0.041, and 0.057 mmol/g, respectively (see Table 1).

For comparison, the Rh(I)-PPh_2-PMO(Ph) was also prepared by traditional grafting method (see Scheme 2) and denoted as Rh(I)-PPh_2-PMO(Ph)-G, where G refers to grafting method. Briefly, 1.0 g of P123 and 3.0 g of KCl were dissolved in 40 mL of 0.067 M HCl aqueous solution, followed by adding 0.99 mL of $(OEt)_3SiPhSi(OEt)_3$ and 0.20 mL of $PPh_2CH_2CH_2$-$Si(OEt)_3$. After being stirred for 24 h at 313 K, the mixture was transferred into an autoclave, followed by hydrothermal treatment at 373 K for another 24 h. The white solid product was filtrated and dried under a vacuum. After being extracted in ethanol solution for 24 h to remove P123 and other organic residues, the as-received PPh_2-PMO(Ph) was added into 10 mL of dry toluene solution containing desired amount of Rh-$(PPh_3)_3Cl$, where the molar ratio between PPh_2-PMO(Ph) and $Rh(PPh_3)_3Cl$ was 1.0:1.0. After stirring for 24 h at room temperature, the solid was centrifuged and dried at 353 K under a vacuum condition, followed by Soxhlet-extraction with

(24) Sheldon, R. A. *Green Chem.* **2005**, *7*, 267–278.
(25) Metivier, P. *Fine Chemicals through Heterogeneous Catalysis*; Wiley-VCH: Weinheim, Germany, 2001.
(26) De Vos, D. E.; Vankelecom, I. F. J.; Jabobs, P. A. *Chiral Catalyst Immobilization and Recycling*; Wiley-VCH: Weinheim, Germany, 2000.
(27) Corma, A. *Chem. Rev.* **1997**, *97*, 2373–2419.
(28) Iwasawa, Y. In *Tailored Metal Catalysts* D. Reidel Publishing Company: Dordrecht, The Netherlands, 1986.
(29) Li, C. *Catal. Rev.* **2004**, *46*, 419–492.
(30) De Vos, D. E.; Dams, M.; Sels, B. F.; Jacobs, P. A. *Chem. Rev.* **2002**, *102*, 3615–3640.
(31) Li, H. X.; Zhang, F.; Wan, Y.; Lu, Y. F. *J. Phys. Chem. B* **2006**, *110*, 22942–22946.
(32) Li, H. X.; Xiong, M. W.; Zhang, F.; Huang, J. L.; Chai, W. *J. Phys. Chem. C* **2008**, *112*, 6366–6371.
(33) Li, H. X.; Zhang, F.; Yin, H.; Wan, Y.; Lu, Y. F. *Green Chem.* **2007**, *9*, 500–505.
(34) Kröcher, O.; Köppel, R. A.; Fröba, M.; Baiker, A. *J. Catal.* **1998**, *178*, 284–298.

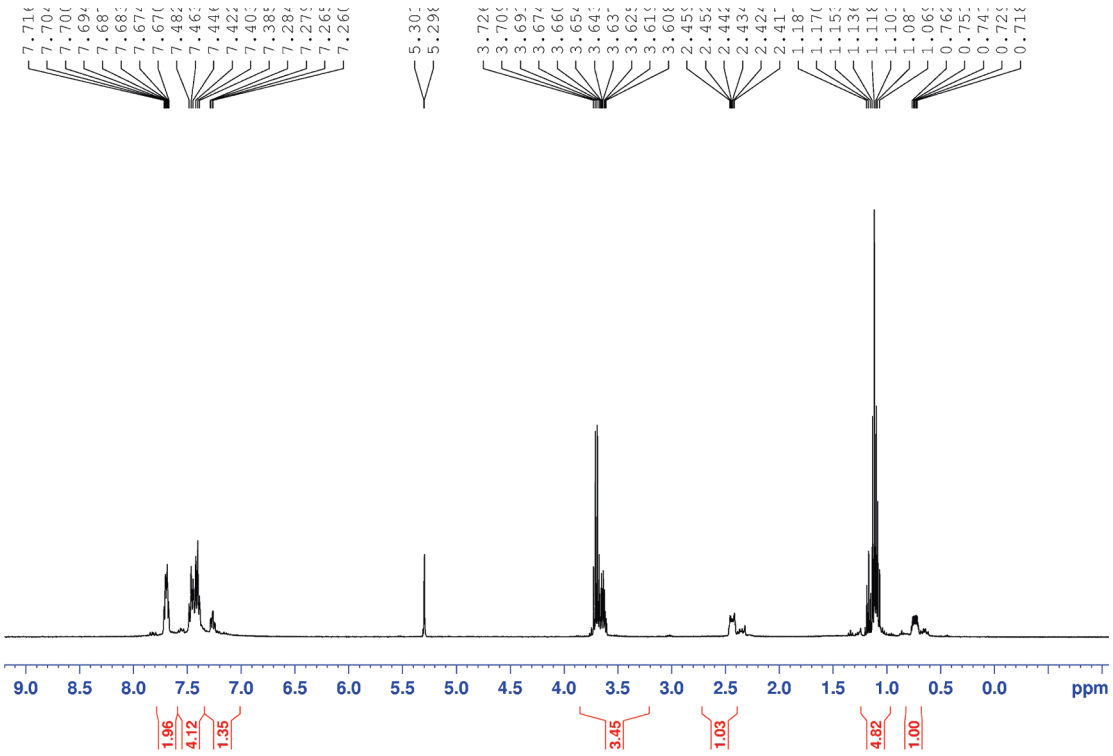

Figure 1. ^{1}H NMR of the RhCl[$PPh_2(CH_2)_2Si(OEt_3)_3$]$_3$ sample in CD_2Cl_2 solution.

Table 1. Structural Parameters and Catalytic Performances of Different Catalysts[a]

			reaction 1			reaction 2		
catalyst	Rh(I) loading (mmol/g)	D_p (nm)	conv. (%)	select. (%)	yield (%)	conv. (%)	select. (%)	yield (%)
Rh(I)-PPh_2-PMO(Ph)-1	0.019	6.4	87	90	78	87	91	79
Rh(I)-PPh_2-PMO(Ph)-2	0.041	5.8	93(90)	90(89)	84(80)	91(89)	93(93)	85(83)
Rh(I)-PPh_2-PMO(Ph)-3	0.057	5.3	81	90	73	84	88	74
Rh(I)-PPh_2-PMO(Ph)-G	0.046	3.6	82(69)	86(87)	71(60)	86(71)	87(87)	75(62)
$Rh(PPh_3)_3Cl$			88	98	86	94	94	88

[a] Conditions for reaction 1: 0.10 mmol of phenylboronic acid, 0.50 mmol of butyl acrylate, a catalyst containing 0.0078 mmol of Rh(I), 6.0 mL of water, and 0.15 mmol ofo n-decane as an internal standard, reaction temperature = 373 K, reaction time = 5 h. Conditions for reaction 2: 0.50 mmol of boronic acid, 0.10 mmol of *N*,*N*-dimehytlacyrlmaide, 1.0 mL of ethanol, 5.0 mL of water, and a catalyst containing 0.0090 mmol of Rh(I) and 0.15 mmol of n-decane as an internal standard, reaction temperature = 373 K, reaction time = 5 h. The values in the parentheses are obtained in the 5th run of recycling tests.

Scheme 2. Illustration of the Preparation of the Rh(I)-PPh_2-PMO(Ph)-G by Grafting Method

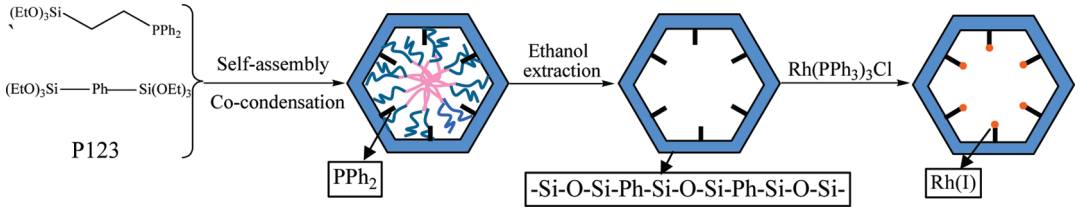

dichloromethane for another 24 h to remove physisorbed Rh(I) species on the support. The Rh(I) loading was determined as 0.046 mmol/g by ICP analysis.

Characterization. Fourier transform infrared (FT-IR) spectra were collected on a Nicolet Magna 550 spectrometer. Small-angle X-ray diffraction (XRD) patterns were obtained on a Rigaku D/maxr B diffractometer with Cu Ka. N_2 adsorption−desorption isotherms were measured at 77 K on a Quantachrome NOVA 4000e analyzer, from which the specific surface area (S_{BET}) was calculated by multiple-point Brunauer−Emmett−Teller (BET) model. The average pore diameter (D_P) was calculated from the adsorption isotherms using Barrett−Joyner−Halenda (BJH) model.[35] Surface morphologies and porous structures were observed through a transmission electron microscopy (TEM, JEOL JEM2011). Solid NMR spectra were recorded on a Bruker DRX-400 NMR spectrometer. The surface electronic states were analyzed by X-ray photoelectron spectroscopy (XPS, Perkin-Elmer PHI 5000C ESCA). All the binding energy values are calibrated by using C_{1S} = 284.6 eV as a reference. The Rh(I)-loading was determined by inductively coupled

(35) Tuysuz, H.; Lehmann, C. W.; Bongard, H.; Tesche, B.; Schmidt, R.; Schuth, F. *J. Am. Chem. Soc.* **2008**, *130*, 11510–11517.

Scheme 3. Chemical Equation of the Reaction between Phenylboronic Acid and Butyl Acrylate (Reaction 1)

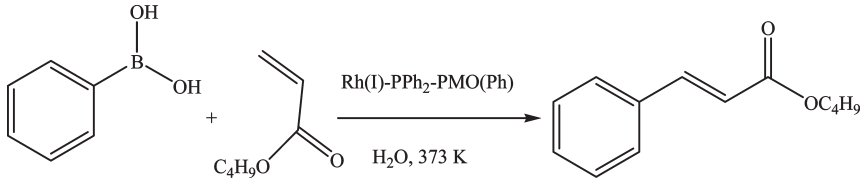

Scheme 4. Chemical Equation of the 1,4-Conjugate Addition Reaction between Phenylboronic Acid and *N*,*N*-Dimehytlacyrlmaide (Reaction 2)

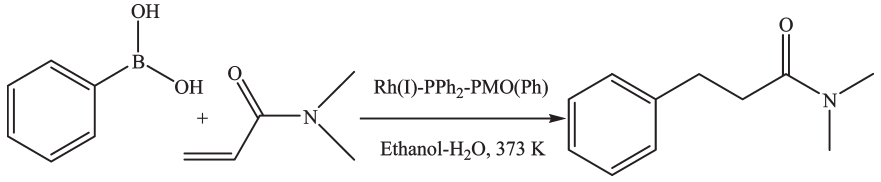

plasma optical emission spectrometer (ICP-OES, Varian VISTA-MPX). Thermal gravimetric analysis (TGA) was performed with a Perkin-Elmer Pyris Diamond TG analyzer under air atmosphere with a heating ramp of 5 K/min.

Activity Test. The reaction between phenylboronic acid and butyl acrylate (reaction 1) and 1,4-conjugate addition reaction between phenylboronic acid and *N*,*N*-dimehytlacyrlmaide (reaction 2) (see Schemes 3 and 4) were used as probes to evaluate the catalytic performances. Reaction 1[18] was carried out at 373 K in a 10 mL round-bottomed flask containing a catalyst with 0.0078 mmol of Rh(I), 0.10 mmol of phenylboronic acid, 0.50 mmol of butyl acrylate, 6.0 mL of distilled water, and 0.15 mmol of n-decane as an internal standard. After stirring for 5 h, the products were extracted by toluene, followed by analysis on a GC-17A gas chromatograph (SHIMADZU) equipped with a JWDB-5, 95% dimethyl 1-(5%)-diphenylpolysiloxane column and a FID detector. The column temperature was programmed from 353 to 523 K at a speed of 10 K/min. N_2 was used as carrier gas. The conversions and yields determined on the GC were calibrated by using commercially available samples, which could also exclude the effect from the trimerization of phenylboronic acid under GC conditions. The selectivity was calculated by dividing the yield with the conversion. Besides the target product (butyl cinnamate), only biphenyl and butyl phenylpropionate were identified as side products in reaction 1. Protodeborylation of phenylboronic acid did not occur because no significant benzene was detected on the GC. To avoid the possible interference from toluene, the products were also extracted by using ethyl acetate, followed by the GC-MS analysis. No significant benzene was detected, which further confirmed the absence of phenylboronic acid protodeborylation during reaction 1. Reaction 2 was carried out at 373 K by stirring a mixture containing a catalyst with 0.0090 mmol of Rh(I), 0.50 mmol of phenylboronic acid, 0.10 mmol of *N*,*N*-dimehytlacyrlmaide, 1.0 mL of ethanol, 5.0 mL of distilled water, and 0.15 mmol of n-decane as an internal standard. After reaction for 5 h, product analysis was performed on the GC under identical conditions. The reproducibility was checked by repeating each result at least three times and is found to be within ±5%.

To determine the catalyst durability, the catalyst was allowed to centrifuge after each run of reactions and the clear supernatant liquid was decanted slowly. The catalyst was washed thoroughly with distilled water and toluene, followed by drying at 353 K for 8 h under vacuum condition. Then, the catalyst was reused with fresh charge of reactants for subsequent recycle under the identical reaction conditions. For comparison, the durability of Rh(I)-PPh_2-PMO(Ph)-2 and Rh(I)-PPh_2-PMO(Ph)-G catalysts was further examined in water-medium reaction 1 at lower conversion by either reducing the catalyst amount from 0.0078 to 0.0039 mmol of Rh(I) or shortening the reaction time from 5 to 3 h.

Results and Discussion

Structural Characteristics. As shown in Figure 2, the FTIR spectra displayed no significant signals indicative of P123, implying that the surfactant was mostly removed after extraction in ethanol. Both the PMO(Ph) and the Rh(I)-PPh_2-PMO(Ph)-2 exhibited three peaks around 654, 1377, and 3050 cm^{-1}, corresponding to the δ(C−H), ν(C−C), and ν(C−H) vibrations from benzene ring.[36] The peaks at 1064 and 1152 cm^{-1} were assigned to the ν(Si−O) and ν(Si−C) vibrations.[37,38] In comparison with PMO(Ph), the Rh(I)-PPh_2-PMO(Ph) displayed three additional absorption peaks at 2980, 2890, and 1438 cm^{-1} characteristic of the ν(C−H) asymmetric and symmetric vibrations from CH_2−CH_2 groups connecting with PPh_2-gropus and the ν(P−C) vibration from the PPh_2-gropus.[39] These results demonstrated the successful incorporation of the Rh(I) organometallic complexes into the network of PMO(Ph) support, which could be further confirmed by solid NMR spectra. As shown in Figure 3, the ^{29}Si MAS NMR spectrum displayed three peaks downfield corresponding to T^1 ($\delta = -64$ ppm), T^2 ($\delta = -74$ ppm), and T^3 ($\delta = -79$ ppm), where $T^m = RSi(OSi)_m\text{-}(OH)_{3-m}$, $m = 1-3$. No Q^n peaks were observed, where $Q^n = Si(OSi)_n\text{-}(OH)_{4-n}$, $n = 2-4$, indicating that all the Si species were covalently bonded with carbon atoms.[11] Meanwhile, the ^{13}C CP MAS NMR spectrum exhibited two peaks around 13 and 31 ppm, which could be assigned to two C atoms in

(36) Wan, Y.; Chen, J.; Zhang, D. Q.; Li, H. X. *J. Mol. Catal.* **2006**, *258*, 89–94.
(37) Huang, H.; Yang, R.; Chinn, D.; Munson, C. *J. Ind. Eng. Chem. Res.* **2003**, *42*, 2427–2433.
(38) Burleigh, M.; Michael, A.; Markowitz, M.; Spector, S.; Gaber, B. *J. Phys. Chem. B* **2001**, *105*, 9935–9942.
(39) Hu, Q. Y.; Hampsey, J. E.; Jiang, N.; Li, C. J.; Lu, Y. F. *Chem. Mater.* **2005**, *17*, 1561–1569.

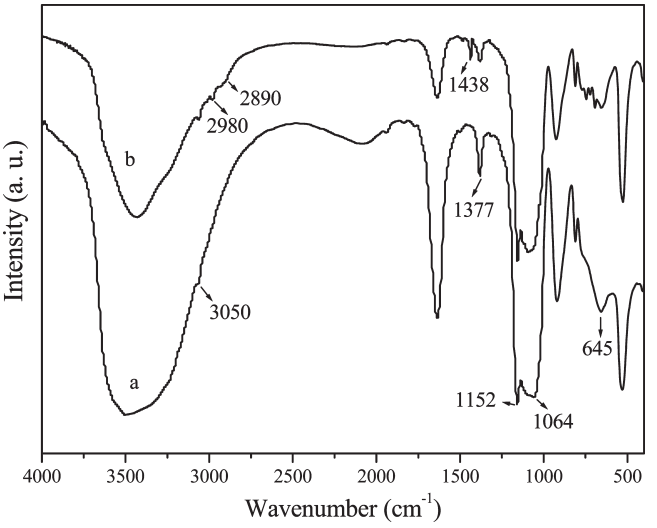

Figure 2. FTIR spectra of (a) PMO(Ph) and (b) Rh(I)-PPh_2-PMO(Ph)-2 samples.

the $-CH_2-CH_2-$ group connecting with the PPh_2-group. An intense peak around 133 ppm was attributable to the C atoms in the benzene ring connected with P the atom in the PPh_2-group or/and embedded in the silica walls. The peak around 58 ppm was assigned to the C atoms in the C_2H_5O-group connecting with Si due to the incomplete hydrolysis.[40] Other peaks denoted by asterisks were attributed to rotational sidebands.[41] A small resonances around 68 ppm and a shoulder for the signal at 80 ppm were observed, implying the presence of trace P123 surfactant in the Rh(I)-PPh_2-PMO(Ph)-2 sample.[42] In addition, the ^{31}P CP MAS NMR spectrum showed a single signal at 39 ppm, corresponding to P atom in the PPh_2-groups. The other peaks could be assigned to rotation side bands because their positions changed with the spinning speed.

Figure 4 shows the TG/DTA curves of the Rh(I)-PPh_2-PMO(Ph)-2 treated in the air. The endothermic peak at 357 K with weight loss around 10% could be attributed to the release of physisorbed water. The exothermic peak around 623 K with weight loss of 12% could be assigned to the oxidation of Rh(I) organometallic complex in the pore channel. The other exothermic peak at 873 K with the weight loss of 27% was resulted from the oxidation of the phenyl fragments embedded in the pore wall.[11] These results also confirmed the successful incorporation of both the Rh(I) organometallic complexes and the phenyl groups onto the silica support.

The XPS spectra (Figure 5) demonstrated that all the Rh species in either the Rh(I)-PPh_2-PMO(Ph)-2 or the $Rh(PPh_3)_3Cl$ sample was present in +1 state.[43] The binding energy of the Rh(I) in the Rh(I)-PPh_2-PMO(Ph)-2 was

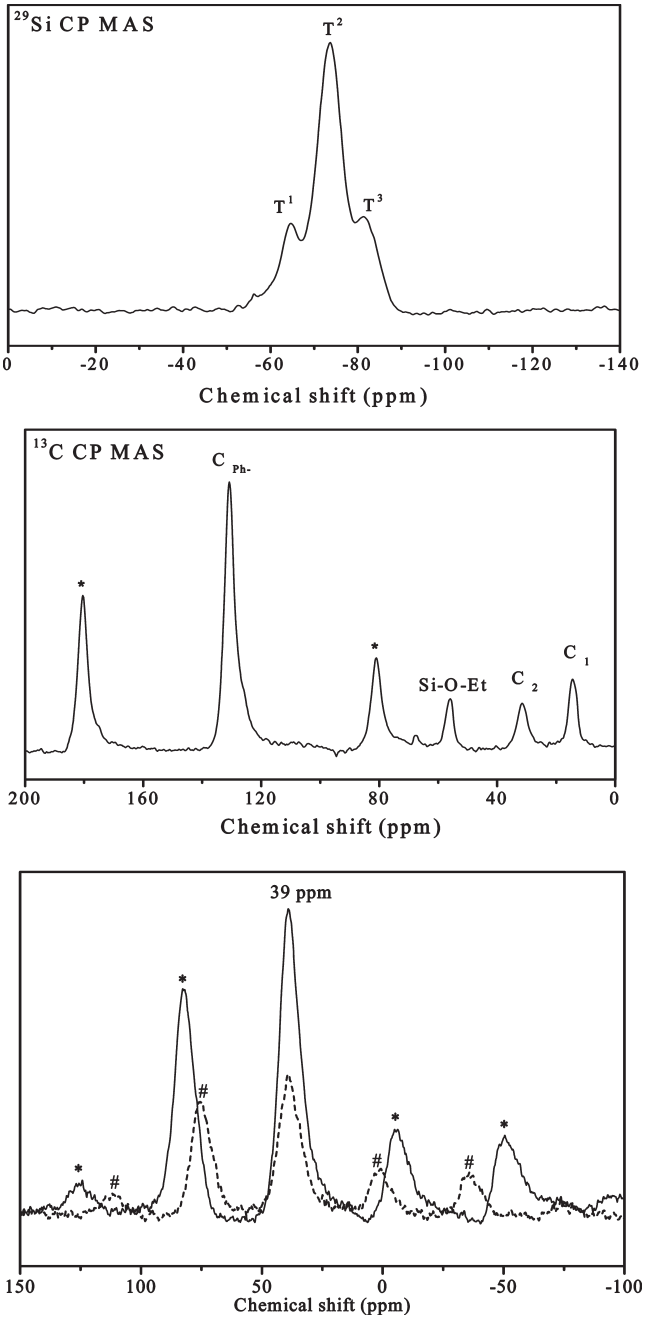

Figure 3. NMR spectra of the Rh(I)-PPh_2-PMO(Ph)-2 sample. Two ^{31}P CP NMR spectra were measured by using different spinning speeds (—— 7 kHz and ----- 5 kHz).

0.6 eV lower than that in the $Rh(PPh_3)_3Cl$. The negative shift of binding energy could be attributed to the stronger electron donation ability of the P atom in the PPh_2-ligand than that in the PPh_3-ligand. This could be easily understood by considering the conjugation Π system between P and Ph, which could dilute the electron density on the P atom. Thus, the P atom in the PPh_3-ligand exhibited lower electron density than that in the PPh_2-CH-CH_2-ligand because of the bigger conjugation Π system, which reduced its electron-donation ability compared to the P atom in the PPh_2-ligand.

Figure 6 revealed that all the Rh(I)-PPh_2-PMO(Ph) samples prepared by either co-condensation or grafting method exhibited typical IV type N_2 adsorption−desorption

(40) Simon, P. F. W.; Ulrich, R.; Spiess, H. W.; Wiesner, U. *Chem. Mater*. **2001**, *13*, 3464–3486.
(41) Posset, T.; Rominger, F.; Blumel, J. *Chem. Mater*. **2005**, *17*, 586–595.
(42) Margolese, J. A.; Melero, S. C.; Christiansen, B. F.; Stucky, G. D. *Chem. Mater*. **2000**, *12*, 2448–2459.
(43) Moulder, J. F.; Stickle, W. F.; Sobol, P. E.; Bomben, K. D. *Handbook of X-ray Photoelectron Spectroscopy, A Reference Book of Standard Spectra for Identification and Interpretation of XPS Data*; Perkin-Elmer Corporation, Physical Electronics Division: Eden Prairie, MN, 1992.

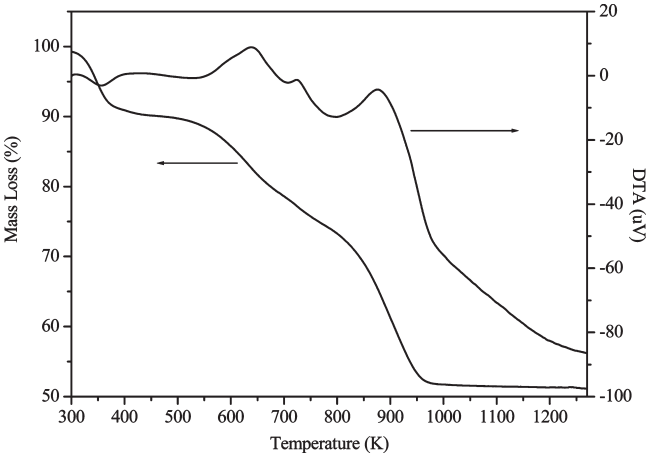

Figure 4. TG/DTA curves of the Rh(I)-PPh_2-PMO(Ph)-2 sample.

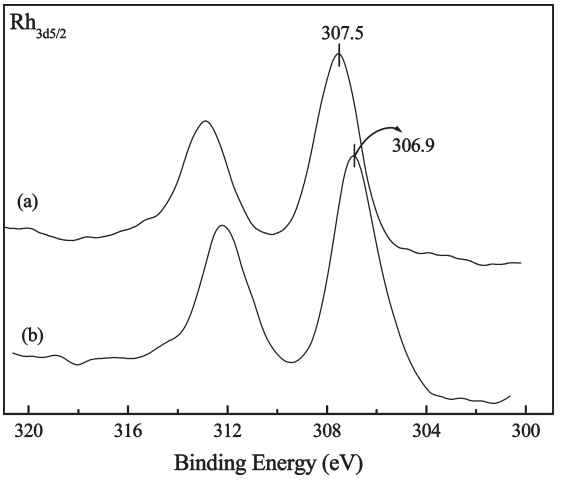

Figure 5. XPS spectra of (a) $Rh(PPh_3)_3Cl$ and (b) Rh(I)-PPh_2-PMO(Ph)-2 samples.

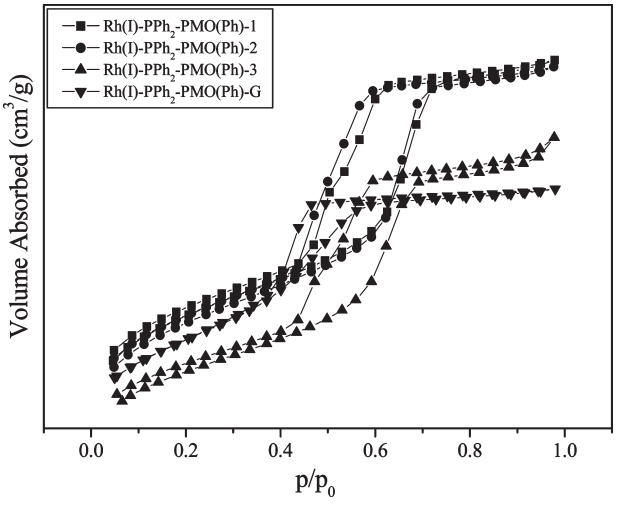

Figure 6. N_2 adsorption−desorption isotherms of Rh(I)-PPh_2-PMO(Ph) samples obtained by co-condensation and grafting methods.

isotherms with a H_1-type hysteresis loop indicative of the mesoporous structure. Meanwhile, the low-angle XRD patterns (Figure 7) displayed an intense diffraction around $2\theta = 0.70°$, indicating the ordered 2D *p6mm* hexagonal mesoporous structures. The magnified XRD pattern showed

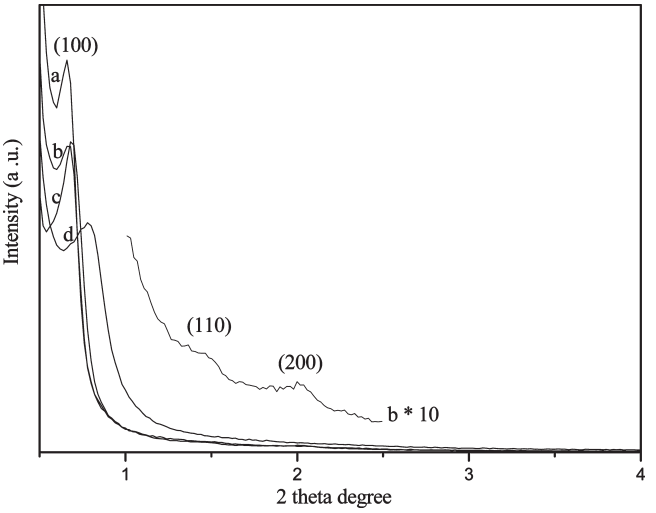

Figure 7. Low-angle XRD patterns of (a) Rh(I)-PPh_2-PMO(Ph)-1, (b) Rh(I)-PPh_2-PMO(Ph)-2, (c) Rh(I)-PPh_2-PMO(Ph)-3, and (d) Rh(I)-PPh_2-PMO(Ph)-G samples.

peaks indicative peaks indicative of (110) and (200) diffractions, suggesting the ordered mesoporous structure, which could be further confirmed by TEM images (Figure 8). The Rh(I)-PPh_2-PMO(Ph)-G exhibited much lower peak intensity than the Rh(I)-PPh_2-PMO(Ph), suggesting that the immobilization of Rh(I) organometallic catalyst by grafting method disturbed the ordering degree of mesoporous structure. The positive shift of peak position demonstrated the increase of wall thickness since the Rh(I) organometallic complexes were mainly anchored on the pore surface in the Rh(I)-PPh_2-PMO(Ph)-G rather than embedded in the pore walls. As shown Table 1, the Rh(I)-PPh_2-PMO(Ph) displayed only very little decrease in the pore diameter (D_P) with the increase of the Rh(I) loading, which further confirmed that the Rh(I) organometallic complexes were mainly embedded in the pore walls and thus had little influence on the pore channels. However, the Rh(I) organometallic complexes in the Rh(I)-PPh_2-PMO(Ph)-G were mainly anchored the pore surface, which partially blocked the pore channels, leading to an abrupt decrease in D_P (see Table 1).

Catalytic Performances. Figure 9 shows the effect of catalyst quantity on the catalytic efficiency in reaction 1. Although the selectivity remained almost constant, the conversion increased almost linearly with the increase of $Rh(PPh_3)_3Cl$ quantity, corresponding to yield increase. The 8.0% catalyst/substrate was employed owing to the maximum yield. Table 1 summarized the catalytic parameters of various catalysts in reaction 1 and reaction 2 conducted in aqueous media. To determine the location of the Rh(I) species, the Rh(I)-PPh_2-PMO(Ph)-2 catalyst was allowed to react with $KMnO_4$ in aqueous solution for enough time. The unreacted $KMnO_4$ was titrated quantitatively by $Na_2C_2O_4$. The Rh(I) content determined $KMnO_4$ oxidation could be considered as these Rh(I) sites accessible for catalytic reactions. The total Rh(I) species were determined by ICP analysis. The experimental results revealed that the molar ratio between Rh(I) species determined by $KMnO_4$ oxidation and total Rh(I) species determined by ICP analysis was

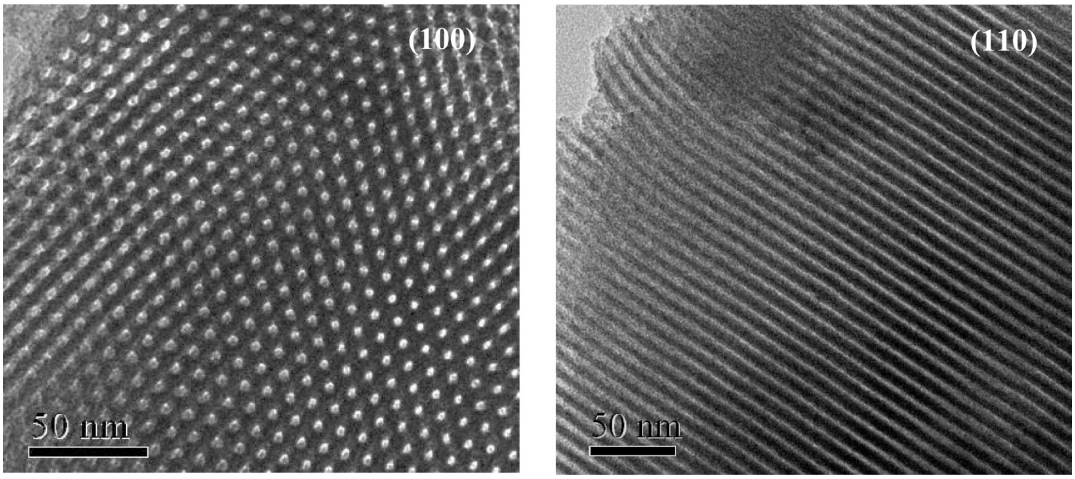

Figure 8. TEM images of the Rh(I)-PPh_2-PMO(Ph)-2 sample along (100) and (110) planes, respectively.

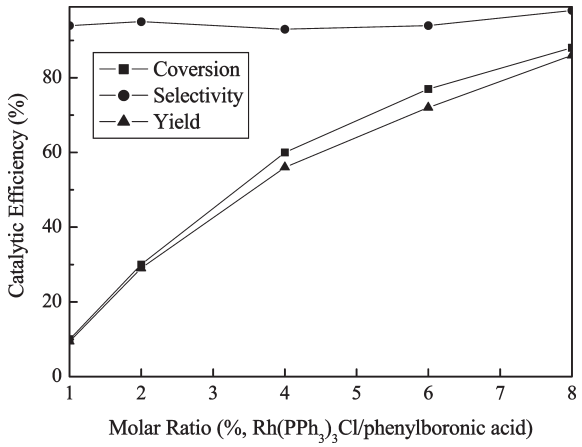

Figure 9. Effect of the quantity of $Rh(PPh_3)_3Cl$ on the reaction efficiency. Reaction conditions: 0.10 mmol of phenylboronic acid, 0.50 mmol of butyl acrylate, 6.0 mL of water, and 0.15 mmol of n-decane as an internal standard, reaction temperature = 373 K, reaction time = 5 h.

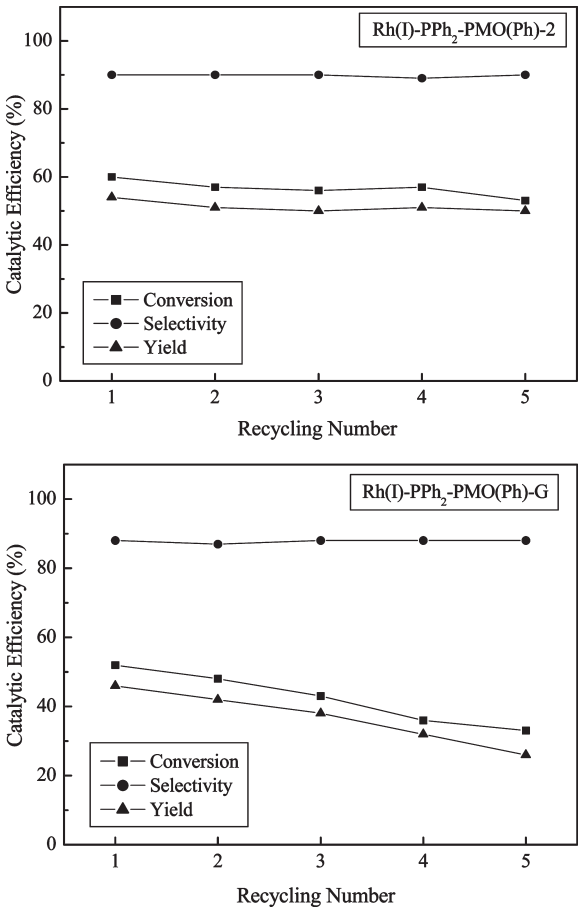

Figure 10. Recycling tests of Rh(I)-PPh_2-PMO(Ph)-2 and Rh(I)-PPh_2-PMO(Ph)-G catalysts in water-medium reaction 1 with the catalyst containing 0.0039 mmol of Rh(I). Other reaction conditions are the same as shown in Table 1.

around 94%, suggesting that most of Rh(I) active sites in the Rh(I)-PPh_2-PMO(Ph)-2 sample were accessible for catalytic reactions. The Rh(I)-PPh_2-PMO(Ph)-G exhibited much lower activity and selectivity than the Rh(I)-PPh_2-PMO(Ph)-2 with the similar Rh(I) loadings. This could be mainly attributed to the narrower pore channel and the lower ordering degree of mesoporous structure, leading to the enhanced diffusion limit. For the Rh(I)-PPh_2-PMO(Ph) series catalysts, the activity first increased and then decreased with the increase in Rh(I) loading while the selectivity remained almost unchanged. The Rh(I)-PPh_2-PMO(Ph)-1 catalyst with very low Rh(I) loading (0.019 mmol/g) exhibited poor activity due to the relatively long distance between the neighboring Rh(I) active sites. Taking into account that either reaction 1 or reaction 2 needed two kinds of molecules adsorbed on the neighboring Rh(I) active sites (see Scheme 3 and 4), the big space between the neighboring Rh(I) active sites would diminish their synergetic effect. Meanwhile, the Rh(I)-PPh_2-PMO(Ph)-3 with very high Rh(I) loading (0.057 mmol/g) also showed poor activity, possibly due to the steric hindrance that retarded the diffusion and even the adsorption of organic molecules on the Rh(I) active sites. The Rh(I)-PPh_2-PMO(Ph)-2 with the Rh(I) loading of 0.041 mmol/g was determined as an optimum catalyst, which exhibited equivalent catalytic efficiencies with the corresponding $Rh(PPh_3)_3Cl$ homogeneous catalyst. To make sure whether the heterogeneous Rh(I) anchored on the support or homogeneous Rh(I) leached from the support was the real catalyst, we carried out the

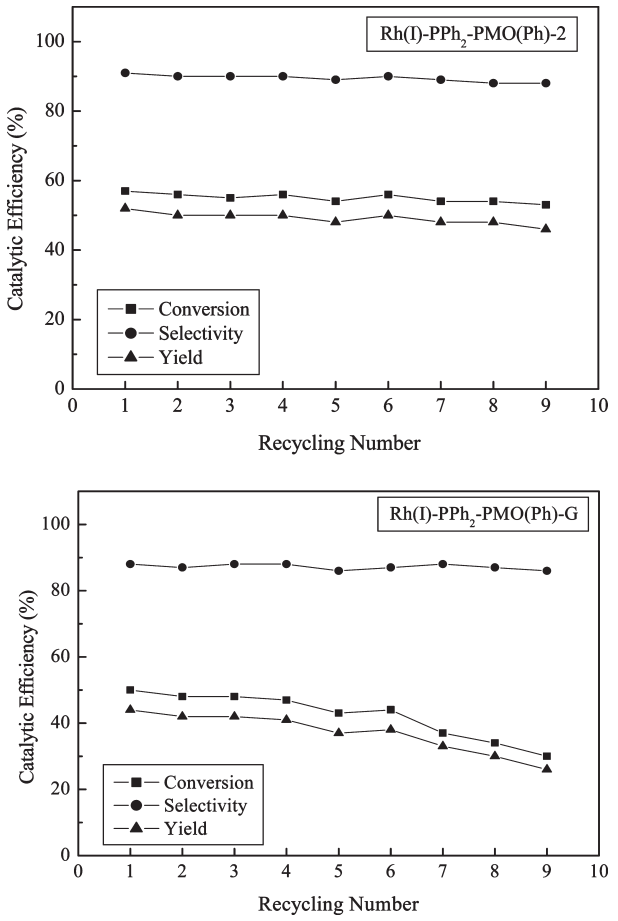

Figure 11. Recycling tests of Rh(I)-PPh_2-PMO(Ph)-2 and Rh(I)-PPh_2-PMO(Ph)-G catalysts in water-medium Reaction 1 with the reaction time of 3 h. Other reaction conditions are given in Table 1.

following experiments according to the procedure proposed by Sheldon et al.[44] When the conversion in reaction 1 reached 30%, the reaction mixture was filtered to remove the solid catalyst and then the mother liquor was allowed to react for another 5 h under the same reaction conditions. No significant change in either the conversion or the yield of product was observed, indicating that the active phase was not the Rh(I) species leached from the supports. Therefore, it is reasonable to conclude that the present catalysis was really heterogeneous in nature.

Besides the durability values listed in Table 1, the durability of Rh(I)-PPh_2-PMO(Ph)-2 and Rh(I)-PPh_2-PMO(Ph)-G catalysts was further examined in water-medium reaction 1 at lower conversion by either reducing the catalyst amount from 0.0078 to 0.0039 mmol of Rh(I) or shortening the reaction time from 5 to 3 h. As shown in Figure 10, when the catalyst containing 0.0039 mmol Rh(I) was employed, the Rh(I)-PPh_2-PMO(Ph)-2 catalyst could be used repetitively 5 times without a significant decrease in catalytic efficiency (conversion, selectivity, and yield) while significant deactivation of the Rh(I)-PPh_2-PMO(Ph)-G was observed after a fifth run of reactions, similar to those observed by using the catalyst

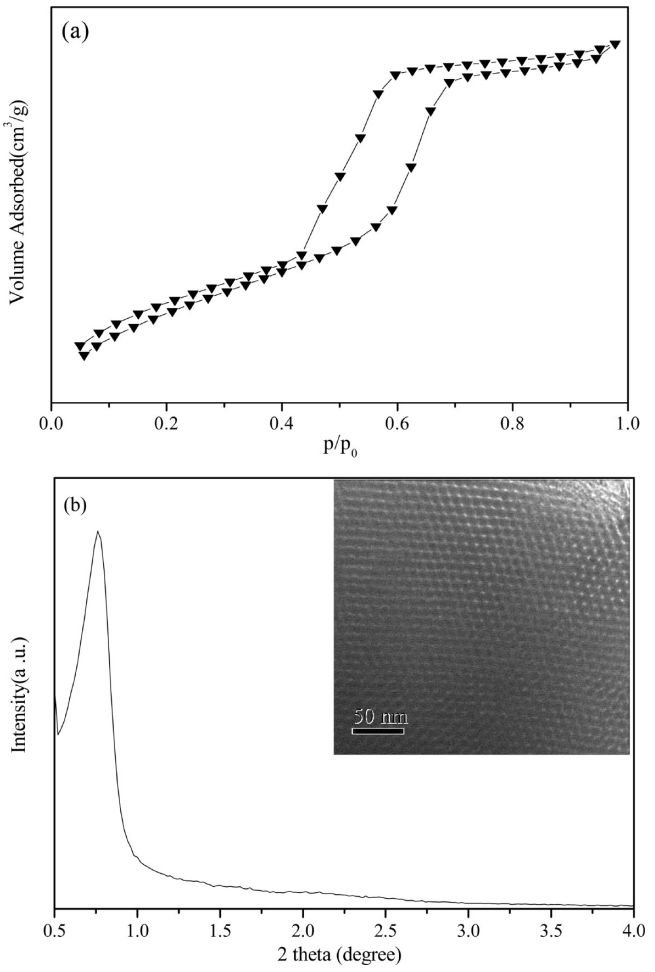

Figure 12. N_2 adsorption−desorption isotherm (a) and the small-angle XRD pattern of the Rh(I)-PPh_2-PMO(Ph)-2 sample after being reused 5 times. The inset is the TEM image.

containing 0.0078 mmol of Rh(I) (see Table 1). Meanwhile, when the reaction time was shortened to 3 h, the Rh(I)-PPh_2-PMO(Ph)-2 could be reused more than 9 times, but the Rh(I)-PPh_2-PMO(Ph)-G could be reused only 6 times (see Figure 11). These results clearly demonstrated that the Rh(I)-PPh_2-PMO(Ph) was more durable than the grafted Rh(I)-PPh_2-PMO(Ph)-G in water-medium organic reactions. The excellent durability of the Rh(I)-PPh_2-PMO(Ph)-2 catalyst could be attributed to the strong interaction of the Rh(I) organometallic complex with the silica support, which could effectively inhibit the Rh(I)-leaching. According to the ICP analysis, Rh(I) species in the solution was less than 0.5 ppm after being used 5 times, suggesting that the Rh(I)-leaching could be essentially neglected. In addition, the Rh(I)-PPh_2-PMO(Ph)-2 catalyst also exhibited strong hydrothermal stability. As shown in Figure 12, the N_2 adsorption−desorption isotherm, XRD pattern and TEM image clearly demonstrated that the Rh(I)-PPh_2-PMO(Ph)-2 remained well-defined ordered mesoporous structure after being reused for 5 times. In contrast, the Rh(I)-PPh_2-PMO(Ph)-G exhibited an abrupt decrease in activity after being used repetitively 5 times. The ICP analysis showed that the Rh(I)-PPh_2-PMO(Ph)-G lost Rh(I) active phase by 15% (atom percentage) after being

(44) Sheldon, R. A.; Wallau, M. I.; Arends, W. C. E.; Schuchardt, U. *Acc. Chem. Res.* **1998**, *31*, 485–493.

used 5 times, suggesting that the Rh(I) species in the Rh(I)-PPh_2-PMO(Ph)-G were more easily leached than those in the Rh(I)-PPh_2-PMO(Ph). Accordingly, the decrease in the activity was mainly attributed to the leaching of Rh(I) active phase. The Rh(I)-PPh_2-PMO-(Ph)-G displayed no significant change in the selectivity to the target products, suggesting that the chemical micro-environment of the Rh(I) active sites remained unchanged.

Conclusions

This work developed a new phenyl and Rh(I) organometal bridged periodic mesoporous organometalsilica catalyst based surfactant-directed co-condensation between RhCl-$[PPh_2(CH_2)_2Si(OEt_3)_3]_3$ and $(OEt)_3SiPhSi(OEt)_3$. In comparison with the grafted Rh(I)-PPh_2-PMO(Ph), the as-prepared framework Rh(I)-PPh_2-PMO(Ph) contained Rh(I) organometallic complexes within the silica framework, which could effectively diminish the blockage of pore channels and the leaching of Rh(I) active phase, leading to higher activity and stronger durability than the grafted Rh(I)-PPh_2-PMO-(Ph) in water-medium reaction between phenylboronic acid and butyl acrylate or the 1,4-conjugate addition reaction between phenylboronic acid and *N*,*N*-dimehytlacyrlmaide. Accordingly, the framework Rh(I)-PPh_2-PMO(Ph) exhibited comparable catalytic efficiencies with the corresponding $Rh(PPh_3)_3Cl$ homogeneous catalyst and could be used repetitively for more than 5 times without significant deactivation. Other periodic mesoporous organometalsilica catalysts including Pd(II), Ru(II), Au(I), Ni(II), etc., could also be designed based on the present method, which may offer more opportunities for designing powerful immobilized homogeneous catalysts for water-medium clean organic reactions.

Acknowledgment. This work was supported by the National Natural Science Foundation of China (20825724), Chinese Education Committee (20070270001), and Shanghai Government (S30406, 07dz22303).